

# Abrupt Flushing of High-Density Core in Internal Diffusion Barrier Plasmas and its Suppression by Plasma Shape Control in LHD

Junichi MIYAZAWA, Ryuichi SAKAMOTO, Satoshi OHDACHI, Masahiro KOBAYASHI, Suguru MASUZAKI, Tomohiko MORISAKI, Satoru SAKAKIBARA, Motoshi GOTO, Shigeru MORITA, Ichihiro YAMADA, Kazumichi NARIHARA, Hisamichi FUNABA, Kenji TANAKA, Clive A. MICHAEL, Yasuhiro SUZUKI, Kiyomasa WATANABE, Nobuyoshi OHYABU, Hiroshi YAMADA, Akio KOMORI, Osamu MOTOJIMA and the LHD experimental group

*National Institute for Fusion Science, 322-6 Oroshi, Toki, Gifu 509-5292, Japan*

(Received 15 November 2007 / Accepted 24 January 2008)

Abrupt flushing of central density occurs in internal diffusion barrier (IDB) plasmas in the Large Helical Device (LHD), where a super dense core (SDC) of the order of  $10^{20} \text{ m}^{-3}$  is formed inside; this event is called “core density collapse (CDC).” CDC must be suppressed as further increase of the central pressure is inhibited. Since CDC is always accompanied by a large Shafranov shift of the plasma center, it has been supposed that mitigation of the Shafranov shift might affect CDC. Vertical elongation of the plasma shape ( $\kappa > 1$ ) is effective in mitigating the Shafranov shift, and  $\kappa$  can be controlled with the quadrupole magnetic field  $B_Q$ . To examine the impact of plasma shape control on CDC,  $B_Q$  scan experiment has been performed in the LHD. The large Shafranov shift in IDB plasmas is mitigated by increasing  $\kappa$ . As a result, CDC is suppressed and high central  $\beta$  values of approximately 7% have been achieved in vertically elongated plasmas. The optimum  $\kappa$  varies with the magnetic configuration. Beta gradients greater than those at CDC in the  $\kappa = 1$  configuration are observed without CDC in vertically elongated plasmas.

© 2008 The Japan Society of Plasma Science and Nuclear Fusion Research

Keywords: heliotron, pellet injection, IDB, SDC, Shafranov shift, beta limit, equilibrium, elongation, MHD instability

DOI: 10.1585/pfr.3.S1047

## 1. Introduction

In toroidal plasmas, the vertical component of a dipole magnetic field induced by the Pfirsch-Schlüter (PS) current  $B_z^{\text{PS}}$  causes the shift of the magnetic axis from  $R_{\text{ax}}$  to  $R_{\text{ax}} + \Delta$ , where  $R_{\text{ax}}$  is the major radius of the magnetic axis in vacuum. This is called the Shafranov shift. Since the PS current is proportional to the pressure gradient,  $\Delta$  is determined by the central plasma beta  $\beta_0$  [1]. Especially in helical plasmas, a large Shafranov shift exceeding a half of the plasma minor radius  $a$  for example, may cause destruction of magnetic surfaces leading to loss of confinement. From this point of view, it is expected that there exists an equilibrium beta limit of  $\Delta \sim 0.5a$  in helical plasmas [2]. Mitigation of Shafranov shift is therefore an important issue to achieve high  $\beta_0$ .

A discovery of internal diffusion barrier (IDB) plasmas in the Large Helical Device (LHD) [3] makes it possible to realize a high central plasma pressure of 1.3 atm [4, 5]. IDB plasmas are produced by hydrogen ice pellet injection and characterized by a strongly peaked den-

sity profile with relatively low density in the edge region, which is called “mantle.” The low mantle density enables deeper penetration of heating beams reaching the plasma center. As long as the central heating power is kept constant, the central pressure increases with the density, following the preferable density dependence of the global confinement scalings, such as ISS95 and ISS04 [6]. IDB plasmas are also characterized by a large Shafranov shift due to high  $\beta_0$ . Recently, a deteriorative phenomenon has been found in IDB plasmas. This phenomenon occurs when the Shafranov shift of the plasma center exceeds a threshold position. Then, the density in the core region is flushed into the mantle region within  $< 1 \text{ ms}$  [7]. We call this event “core density collapse (CDC)” [4, 5]. CDC must be suppressed since it prevents further increase of the central pressure and the fusion triple product. Since CDC is always accompanied by a large Shafranov shift, its mitigation might affect CDC.

At least three methods are effective for Shafranov shift mitigation, i.e., 1) plasma position control with the vertical magnetic field that compensates  $B_z^{\text{PS}}$ , 2) increase of the rotational transform ( $\iota$ ), and 3) vertical elongation of

author's e-mail: miyazawa@LHD.nifs.ac.jp

the plasma shape. The first method is straightforward and will be effective only if it is applied with the feedback control. Use of a strong vertical field from the beginning of a discharge is not preferable, because the initial magnetic configuration shifts strongly inward and MHD instabilities are expected to be unstable in such configurations [8]. Unfortunately, feedback control of the vertical field is not yet equipped on the LHD, although it is under discussion as a future program (available magnetic field strength is, however, expected to be low). As for the second method, this works as reported in [9]. The PS current (and therefore  $B_z^{\text{PS}}$ ) is inversely proportional to  $\iota$  and as a result,  $\Delta \propto B_z^{\text{PS}}/\iota \propto 1/\iota^2$ . In the LHD,  $\iota$  can be controlled by changing the magnetic configuration, and increases with the aspect ratio of the torus. However, the maximum magnetic field strength in high aspect ratio configurations is limited to  $\sim 1$  T. Therefore, the third method of vertical elongation is the only possible solution available at the maximum magnetic field strength of  $\sim 3$  T.

The plasma shape control has been usually applied in tokamaks and the majority of modern and future tokamaks have vertically elongated cross sections. The plasma shape control is also effective in helical plasmas, as was shown in the Advance Toroidal Facility (ATF) [10, 11] and LHD [12]. In ATF, the bootstrap current was controlled by changing the plasma shape [11]. The effects of plasma elongation and rotational transform on the Shafranov shift were already investigated in LHD [12]. The experiment was conducted using plasmas with relatively flat pressure profiles, in an inward shifted magnetic configuration of  $R_{\text{ax}} = 3.6$  m. Therefore, high beta plasmas with strongly peaked pressure profiles, such as IDB plasmas observed in the outward shifted configurations ( $R_{\text{ax}} > 3.70$  m), were not covered in [12].

In this paper, experimental results of the elongation scan and its impact on CDC are reported. The method of plasma shape control is described in Section 2. A brief review of CDC is provided in Section 3. Experimental results of the plasma shape control aimed at CDC suppression are provided in Section 4. Possible causes of CDC are discussed in Section 5. Section 6 is a summary.

## 2. Plasma Shape Control by the Quadrupole Magnetic Field

In toroidal plasmas, the PS current induced cancels the charge separation due to variation in the magnetic field strength  $\Delta B$  on flux surfaces, which is proportional to  $1/R$ . Therefore, vertical elongation, which reduces the characteristic length of the torus in the major radius direction  $\Delta R$ , is also effective in reducing  $\Delta B \propto \Delta R$  and the PS current. The magnetic surfaces in heliotron plasmas with a pole number of  $l = 2$  as in LHD can be approximated by a rotating ellipse, i.e., horizontally and vertically elongated ellipses appear alternately as the toroidal angle increases. Plasma elongation  $\kappa$  is defined as the toroidally

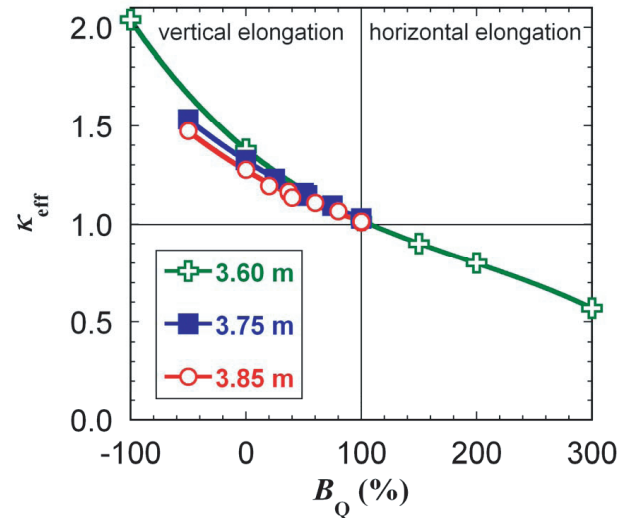


Fig. 1 Relation between the quadrupole magnetic field  $B_Q$  and the effective plasma elongation  $\kappa_{\text{eff}}$  in low beta plasmas of  $R_{\text{ax}} = 3.75$  m (filled squares) and  $3.85$  m (circles). LCFS elongation estimated from the vacuum magnetic data for  $R_{\text{ax}} = 3.60$  m, except the point at  $B_Q = 150\%$  where  $\kappa_{\text{eff}}$  is measured, is also shown (crosses).

averaged ratio of the minor radius in the vertical direction to that in the major radius direction of the last closed flux surface (LCFS). In LHD, we measure two kinds of line density,  $nL_{\text{FIR}}$  and  $nL_{\text{MMW}}$ , passing through the “major axes” of vertically and horizontally elongated ellipses, using a far-infrared (FIR) interferometer and a millimeter wave (MMW) interferometer, respectively. Here, we define an effective elongation  $\kappa_{\text{eff}} \equiv nL_{\text{FIR}}/nL_{\text{MMW}}$ . Note that these line densities include the information outside the LCFS (called ergodic region), and therefore,  $\kappa_{\text{eff}}$  is an approximation of  $\kappa$ .

Both in helical plasmas and tokamaks,  $\kappa$  is controlled by the quadrupole magnetic field  $B_Q$  [1]. In the standard configurations of LHD, the quadrupole component generated by two helical coils is 100% cancelled by the quadrupole field generated by poloidal coils and therefore  $\kappa = 1$ . Hereinafter,  $B_Q$  that results in  $\kappa = 1$  is called “ $B_Q = 100\%$ .” When  $B_Q$  is decreased to  $< 100\%$ ,  $\kappa$  becomes larger than 1, i.e., the plasma is vertically elongated. The relation between  $B_Q$  and  $\kappa_{\text{eff}}$  in low beta plasmas at  $R_{\text{ax}} = 3.75$  m and  $3.85$  m is shown in Fig. 1. The elongation of the LCFS estimated from the vacuum magnetic data for  $R_{\text{ax}} = 3.60$  m is also shown in Fig. 1 (the point at  $B_Q = 150\%$  is measured). Although  $\kappa_{\text{eff}}$  includes the information of the ergodic region, it approximates the elongation of the LCFS well.

Theoretically,  $\Delta$  is expressed as [13]

$$\Delta = \frac{R_0 \beta_0}{4(\iota/2\pi)^2 f(\kappa)}, \quad (1)$$

for low beta, shearless (flat  $\iota$ ), and fixed boundary case, where  $\iota = 2\pi\epsilon$  is the rotational transform,  $\kappa$  is the plasma

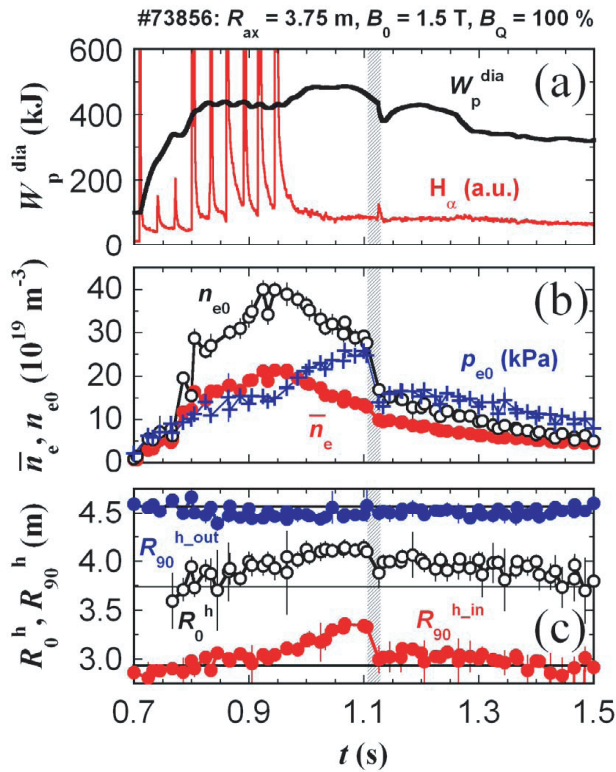


Fig. 2 Typical waveforms in an IDB discharge, where (a) the diamagnetic stored energy  $W_p^{\text{dia}}$  and the  $H_\alpha$  intensity, (b) the central electron density  $n_{e0}$ , the central electron pressure  $p_{e0}$ , and the line-averaged electron density, (c) positions of the plasma center  $R_0^h$  and the inboard (outboard) side plasma edge  $R_{90}^{\text{h,in}}$  ( $R_{90}^{\text{h,out}}$ ), where  $\beta = 0.1\beta_0$ , on the equatorial plane of a horizontally elongated cross section, are shown from top to bottom. CDC occurs at  $t \sim 1.13$  s.

elongation ( $\kappa > 1$  for vertical elongation), and  $f(\kappa)$  is given by

$$f(\kappa) = \frac{1}{2} \left( \kappa + \frac{1}{\kappa} \right) \sqrt{\kappa}. \quad (2)$$

The Shafranov shift can be effectively mitigated by increasing the rotational transform and/or plasma elongation, as can be seen in Eq. (1).

### 3. Core Density Collapse Event

A super-dense core of the order of  $10^{20} \text{ m}^{-3}$  is formed inside the IDB during the recovery phase of the central pressure after pellet injection in LHD, which is called as “reheat” [3,4]. Waveforms in a typical IDB discharge are shown in Fig. 2. A large Shafranov shift of the plasma center measured on a horizontally elongated cross section,  $R_0^h = R_{\text{ax}} + \Delta$ , is observed during the recovery phase ( $t = 0.95$ - $1.12$  s) and the shift  $\Delta$  reaches approximately 50 % of the plasma minor radius. An abrupt flushing of the central density is observed at  $t \sim 1.13$  s, which is called CDC. This event finishes within  $< 1$  ms, according to the fast soft X-ray measurement [7] (not shown). At CDC,  $R_0^h$

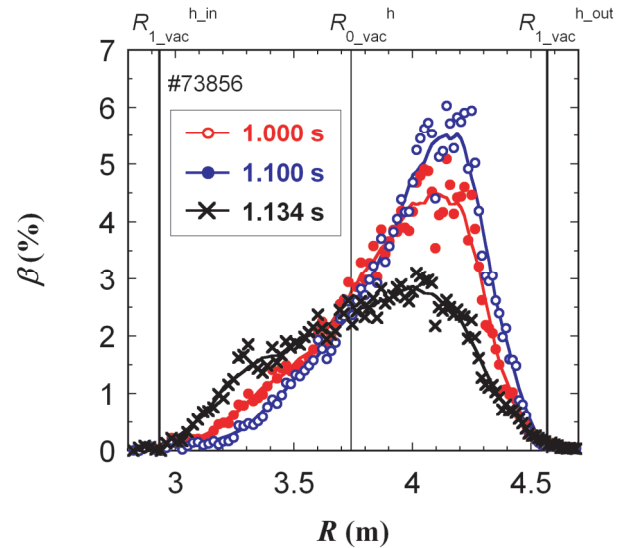


Fig. 3 Temporal change of the plasma beta profile on the equatorial plane of a horizontally elongated cross section, measured by Thomson scattering, in the discharge shown in Fig. 2. Vertical lines denote radial positions of the inboard (outboard) side LCFS  $R_{1,\text{vac}}^{\text{h,in}}$  ( $R_{1,\text{vac}}^{\text{h,out}}$ ) and the magnetic axis  $R_{0,\text{vac}}^{\text{h}}$  in vacuum.

exceeds  $\sim 4.1$  m. This threshold position is insensitive to the initial magnetic configuration, at least for  $R_{\text{ax}} = 3.75$ - $3.90$  m.

Radial profiles of the plasma pressure (beta) before and after CDC are shown in Fig. 3, which are measured by Thomson scattering and obtained from the same discharge in Fig. 2. The plasma center shifts outward (from left to right in Fig. 3) as the central beta increases from  $\sim 4.5\%$  ( $t = 1.0$  s) to  $\sim 5.5\%$  ( $t = 1.1$  s). At the same time, the inboard side plasma edge also shifts outward (see also  $R_{90}^{\text{h,in}}$  in Fig. 2(c), which denotes the inboard side radial position of  $\beta = 0.1\beta_0$ ). Immediately after CDC ( $t = 1.134$  s), both the plasma center and the inboard side edge move inward, and the pressure profile changes from strongly peaked to approximately parabolic. It should be noted that the temperature profile is hardly affected by CDC [4,7]. This is the reason why we call this “density collapse.” Compared with the plasma center position, which is difficult to be strictly determined (in this study,  $R_0^h$  is given as the average position of the ten points with the highest beta in the Thomson profile data), it is easier to determine  $R_{90}^{\text{h,in}}$  due to the steep slope around there. Hereinafter, both  $R_0^h$  and  $R_{90}^{\text{h,in}}$  will be used to measure the Shafranov shift.

### 4. CDC Suppression by Vertical Elongation

As was explained in Section 2, plasma elongation is controlled by the quadrupole field  $B_Q$ . Vertical elongation with  $B_Q < 100\%$ , which results in  $\kappa_{\text{eff}} > 1$  (see Fig. 1), mitigates the PS current and thus the Shafranov shift. In Fig. 4,

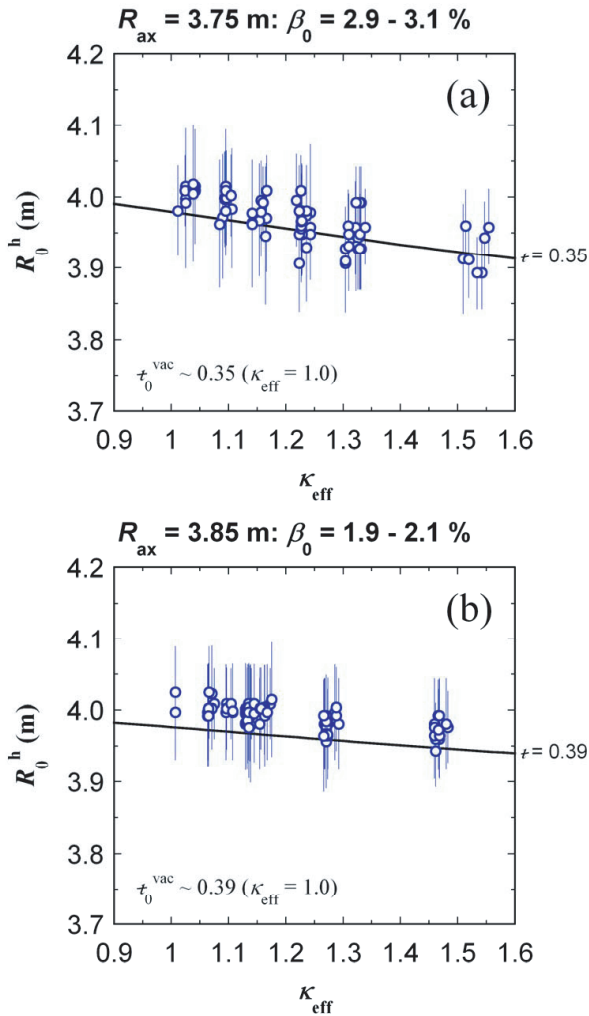


Fig. 4 Shafranov shift dependence on  $\kappa_{\text{eff}}$  in low beta plasmas for (a)  $R_{\text{ax}} = 3.75$  m and (b) 3.85 m, measured by Thomson scattering.  $R_0^h$  is the magnetic axis position measured at a horizontally elongated cross section and lines denote the theoretical prediction of Eq. (1).  $\tau_0^{\text{vac}}$  inside the figure corresponds to the minimum  $\tau$  in the  $\kappa_{\text{eff}} \sim 1.0$  configuration in vacuum.

the Shafranov shift dependence on  $\kappa_{\text{eff}}$  in low beta plasmas is shown, where the theoretical prediction of Eq. (1) is also plotted. Note that a flat  $\tau$  profile is assumed in Eq. (1). On the other hand,  $\tau$  increases monotonically from the center ( $< 0.5$ ) to the edge ( $> 1$ ) in low beta plasmas of the LHD. Therefore,  $\tau_0^{\text{vac}}$ , which is the rotational transform at the plasma center in vacuum, corresponds to the minimum  $\tau$  that has a large influence on the Shafranov shift. In spite of the difference in the  $\tau$  profile, the theoretical prediction agrees well with the experimental results. In other words, the Shafranov shift is indeed mitigated in vertically elongated plasmas as predicted by the theory. This effect is also recognized in high beta plasmas shown in Fig. 5, where radial beta profiles of  $B_Q = 100\%$  ( $\kappa_{\text{eff}} \sim 1.0$ ), which are identical to that shown in Fig. 3 ( $t = 1.1$  s), and  $B_Q = 25\%$  ( $\kappa_{\text{eff}} \sim 1.2$ ) are depicted. Although  $\beta_0$  of  $\sim 5.5\%$  is sim-

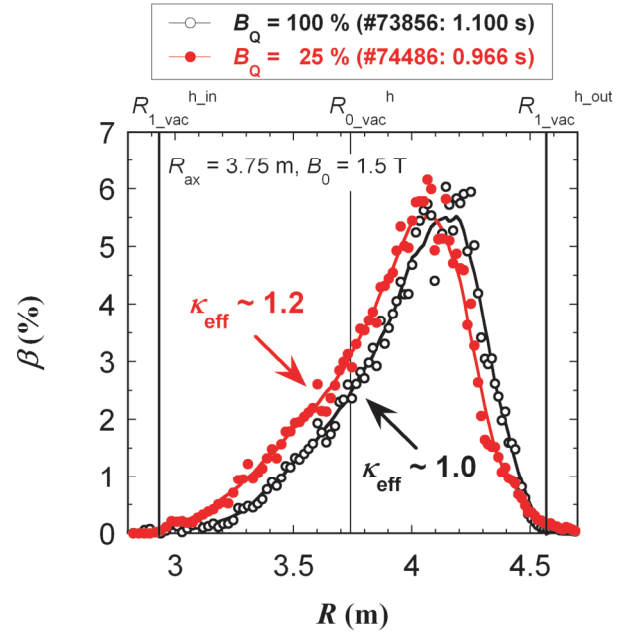


Fig. 5 Comparison of the plasma beta profiles measured by Thomson scattering on the equatorial plane of a horizontally elongated cross section, in two discharges with  $B_Q = 100\%$  ( $\kappa_{\text{eff}} \sim 1.0$ ) and  $B_Q = 25\%$  ( $\kappa_{\text{eff}} \sim 1.2$ ). Vertical lines denote radial positions of the inboard (outboard) side LCFS  $R_{1\_vac}^{h\_in}$  ( $R_{1\_vac}^{h\_out}$ ) and the magnetic axis  $R_{0\_vac}^h$  in vacuum.

ilar for both the cases, the Shafranov shift of the plasma center is smaller in the case of  $B_Q = 25\%$ . The impact of vertical elongation is clearly observed at the positions of the plasma center and the inboard (left-hand) side plasma edge, while the position of the outboard (right-hand) side plasma edge is fixed.

Shafranov shift dependence on  $\beta_0$  at various  $B_Q$  is shown in Fig. 6(a). A large difference between  $B_Q = 100\%$  and  $25\%$  is recognized at high  $\beta_0$  of over  $3\%$ . Compared with  $\beta_0 \sim 5.5\%$ ,  $R_0^h$  reaches  $\sim 4.15$  m and CDC occurs in the case of  $B_Q = 100\%$ , while  $R_0^h$  is below 4.1 m and no CDC is observed in the case of  $B_Q = 25\%$ . Also shown in Fig. 6(a) is the data obtained in an intermediate case of  $B_Q = 53\%$ , where  $B_0$  is decreased to 1.0 T to achieve higher  $\beta_0$  under a limited heating power condition of  $\sim 10$  MW. In this case,  $R_0^h$  is  $\sim 4.1$  m at  $\beta_0 \sim 5\%$  and reaches  $\sim 4.15$  m at  $\beta_0 > 6\%$ . The highest  $\beta_0$  of  $\sim 7\%$  is achieved without CDC in this configuration. The influence of vertical elongation is also recognized for the inboard side plasma edge position  $R_{90}^{h\_in}$ , as shown in Fig. 6(b). CDC occurs when  $R_{90}^{h\_in}$  reaches  $\sim 3.35$  m at  $\beta_0 \sim 5.5\%$ , in the case of  $B_Q = 100\%$ . In cases of small  $B_Q$ ,  $R_{90}^{h\_in}$  remains less than 3.35 m even with high  $\beta_0$  of  $> 6\%$ . It is expected that CDC will also occur in vertically elongated plasmas as in the case of  $B_Q = 100\%$ , but at higher  $\beta_0$ . However, the higher  $\beta_0$  regime of  $> 7\%$  remains to be explored in a future study.

Results of the  $B_Q$  scan experiment are summarized in

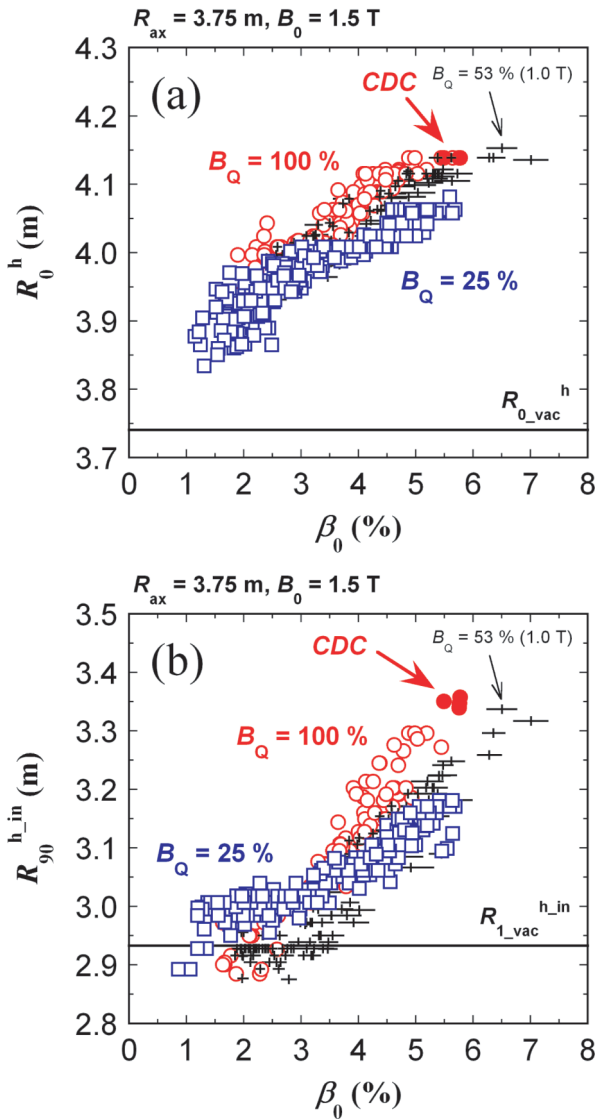


Fig. 6 Central beta dependence of (a) the plasma center  $R_0^h$  and (b) the inboard side plasma edge  $R_{90}^{h,in}$ , where  $\beta = 0.1 \beta_0$  on the equatorial plane of a horizontally elongated cross section. The magnetic field strength  $B_0$  is 1.5 T in the cases of  $B_Q = 100\%$  (circles) and 25% (squares), and  $B_0 = 1.0$  T in the case of  $B_Q = 53\%$  (crosses with horizontal error bar). Filled circles denote the data just before CDC.

Fig. 7, where the  $\kappa_{eff}$  dependence of the inboard side edge position  $R_{90}^{h,in}$  is shown for various sets of different  $\beta_0$ . At low  $\beta_0$  ( $< 2\%$ ),  $R_{90}^{h,in}$  increases monotonically with  $\kappa_{eff}$ , reflecting the vertical elongation effect. A nonlinear response of  $R_{90}^{h,in}$  is recognized in high beta datasets of  $\beta_0 > 2\%$ . The optimum  $\kappa_{eff}$  to keep  $R_{90}^{h,in}$  apart from the CDC threshold in high beta plasmas varies with the initial magnetic configuration, e.g., it is  $\sim 1.2$  for  $R_{ax} = 3.75$  m and  $\sim 1.3$  for  $R_{ax} = 3.85$  m. It would be better to avoid excess elongation than the optimum  $\kappa_{eff}$ , because the confinement volume becomes smaller.

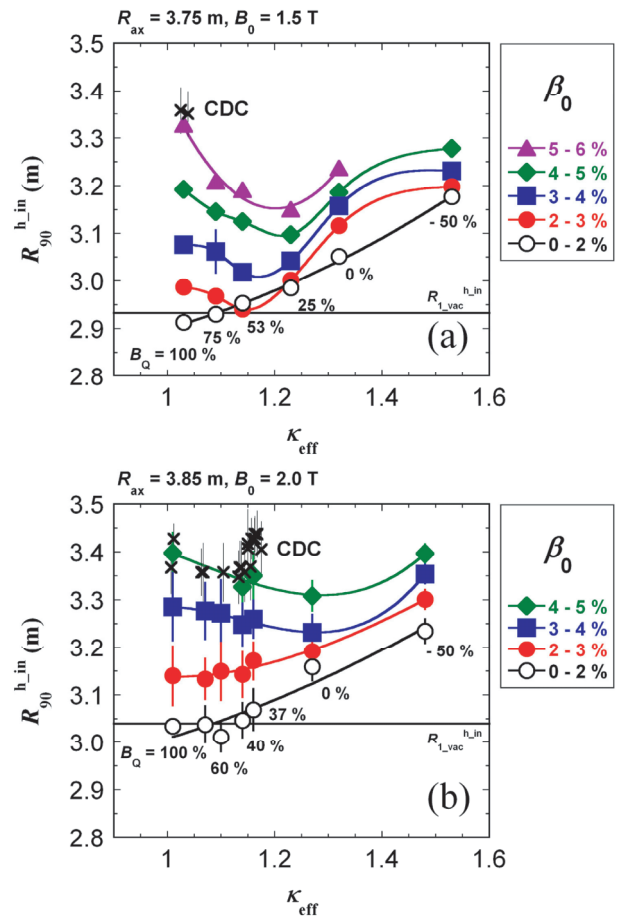


Fig. 7 Parametric plots of  $R_{90}^{h,in}$  versus  $\kappa_{eff}$  for (a)  $R_{ax} = 3.75$  m and (b)  $R_{ax} = 3.85$  m, where  $\beta_0$  is used as the parameter. Crosses denote the position where CDC occurs.

### 5. Discussion

It has been shown that plasma elongation is effective for Shafranov shift mitigation. No CDC is observed as long as the shift of the plasma center (or the inboard side plasma edge) is kept apart from the threshold position. In this sense, CDC seems to be related to the equilibrium limit. On the other hand, it is widely believed that the equilibrium limit will appear as a “soft limit” as seen in [2], where no fast event such as CDC is expected. From this point of view, MHD instabilities should be considered as the cause of CDC. Basically, the ideal interchange mode frequently observed in the inward shifted configurations ( $R_{ax} < 3.65$  m) [14, 15], which is independent of the mode numbers, is being stabilized in the outward shifted configurations [7, 16], where IDB plasmas are easily formed. This stability increases with the Shafranov shift due to the self-formation of the magnetic well [3]. In vertically elongated plasmas, however, the Shafranov shift is mitigated and the self well formation effect becomes weak, resulting in stability degradation. Therefore, the ideal interchange mode, which can be destabilized in vertically elongated plasmas, is not the cause of CDC that is stabilized by vertical elon-

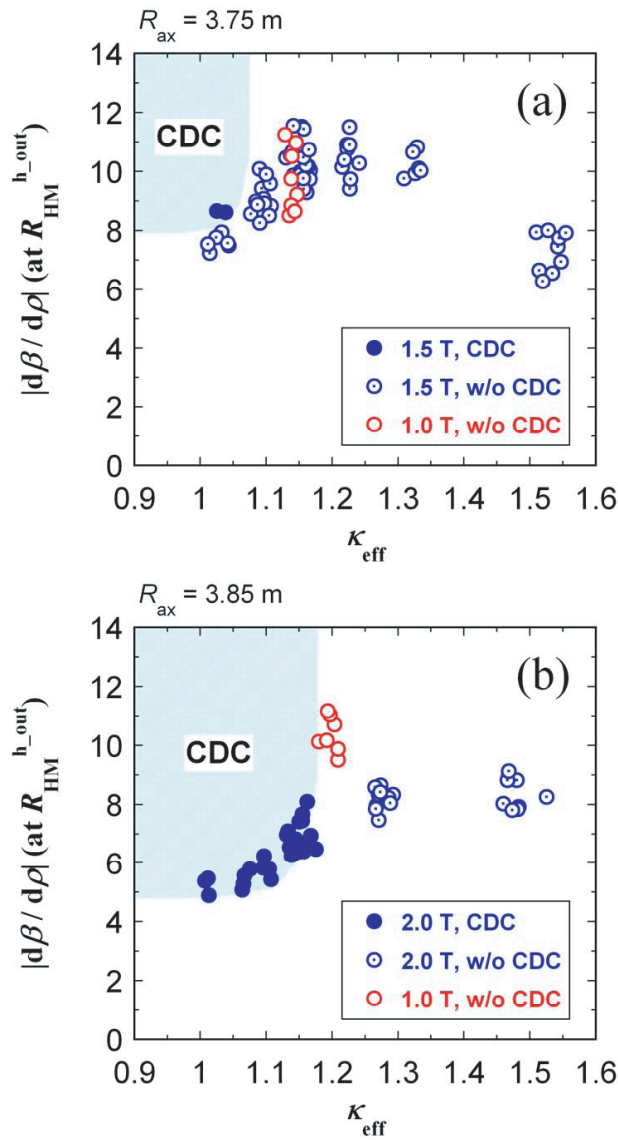


Fig. 8 The normalized beta gradient  $|\frac{d\beta}{d\rho}|$  at  $R_{HM}^{h_{out}}$ , where  $\beta = 0.5 \beta_0$  in the outboard side of a horizontally elongated cross section, versus  $\kappa_{eff}$  for (a)  $R_{ax} = 3.75$  m and (b)  $R_{ax} = 3.85$  m. The beta gradient  $|\frac{d\beta}{dR}|$  is estimated from the profile data of the Thomson scattering and then normalized by  $(R_{98}^{h_{out}} - R_0^h)$  as  $|\frac{d\beta}{d\rho}| = |\frac{d\beta}{dR}| \times (R_{98}^{h_{out}} - R_0^h)$ , where  $R_{98}^{h_{out}}$  is the position of  $\beta = 0.02 \beta_0$  in the outboard side of a horizontally elongated cross section. CDC occurs in the hatched region.

gation.

There still is a possibility of CDC being caused by other instabilities, such as the resistive [17] and ballooning modes, which have not yet been considered in detail under realistic conditions. The instability, if it really exists, should have a characteristic that it is stabilized in vertically elongated configurations. High  $\beta_0$  of  $\sim 7\%$ , which is higher than that observed at CDC, is achieved in vertically elongated plasmas without CDC. It should also be noted that in vertically elongated plasmas, the maximum

pressure gradient observed in the experiment, which might be the energy source of this instability, is larger than those at CDC in the  $\kappa_{eff} \sim 1$  configurations, as shown in Fig. 8. In the figure, the maximum beta gradient at  $R_{HM}^{h_{out}}$ , where  $\beta = 0.5 \beta_0$  at the outboard side on a horizontally elongated cross section, is plotted against  $\kappa_{eff}$ . Especially in the case of  $R_{ax} = 3.85$  m shown in Fig. 7(b), the beta gradient at CDC increases with  $\kappa_{eff}$ , and finally, no CDC is observed at  $\kappa_{eff} > 1.18$ . This suggests that the instability causing CDC has thresholds in both the beta gradient and  $\kappa_{eff}$ , i.e., the CDC should have been stabilized in vertically elongated plasmas with  $\kappa_{eff}$  larger than the threshold.

## 6. Summary

Shafranov shift mitigation by plasma shape control has been performed in LHD. The CDC event that prevents further increase of the central pressure in IDB plasmas has been stabilized in vertically elongated configurations, where the Shafranov shift is mitigated. As a result, high central beta values of  $\sim 7\%$  are achieved in IDB plasmas. It has also been shown from the results of the elongation scan experiment that there is an optimum value of plasma elongation depending on the initial magnetic configuration. Although the physics scenario describing CDC is not concluded here, it is suggested that the instability causing CDC, if exists, may have the following characteristics: 1) the critical beta gradient activating the instability increases with the elongation, and 2) the instability becomes stabilized in vertically elongated plasmas with  $\kappa$  larger than the threshold, which varies with the magnetic configuration.

## Acknowledgments

The authors would like to thank the staff of LHD for valuable discussions and for supporting the experiments in this device. They are grateful to Dr. J. Geiger for providing the theoretical expression of the Shafranov shift. This work is supported by NIFS07ULPP517.

- [1] V.D. Pustovitov, *Reviews of Plasma Physics Vol.21* (Consultants Bureau, New York, 2000) p.1-201.
- [2] A. Weller *et al.*, *Plasma Phys. Control. Fusion* **45**, A285 (2003).
- [3] N. Ohya *et al.*, *Phys. Rev. Lett.* **97**, 055002 (2006).
- [4] H. Yamada *et al.*, *34th European Physical Society Conferences on Plasma Physics 2007 (Warsaw, Poland)*, I4.004, to be published in *Plasma Phys. Control. Fusion*.
- [5] R. Sakamoto *et al.*, to be published in *Plasma and Fusion Research*.
- [6] H. Yamada *et al.*, *Nucl. Fusion* **45**, 1684 (2005).
- [7] S. Ohdachi *et al.*, "MHD instabilities with sharply peaked pressure profile after ice-pellets injection in the Large Helical Device," *Proceedings of the Joint Conference of 17th International Toki Conference and 16th International Stellarator/Heliotron Workshop*, P1-051 (2007).
- [8] O. Kaneko *et al.*, *Phys. Plasmas* **9**, 2020 (2002).
- [9] O. Motojima *et al.*, *Nucl. Fusion* **45**, S255 (2005).

- [10] B.A. Carreras *et al.*, Nucl. Fusion **24**, 1347 (1984).  
[11] R.J. Colchin *et al.*, Phys. Fluids **B2**, 1347 (1990).  
[12] T. Kobuchi *et al.*, Plasma Phys. Control. Fusion **48**, 789 (2006).  
[13] J. Geiger, private communication.  
[14] S. Sakakibara *et al.*, Nucl. Fusion **45**, S255 (2005).  
[15] S. Sakakibara *et al.*, Nucl. Fusion **45**, S255 (2005).  
[16] Y. Narushima *et al.*, “3-D ideal MHD stability of super dense core plasma in LHD,” Proceedings of the Joint Conference of 17th International Toki Conference and 16th International Stellarator/Heliotron Workshop, P1-053 (2007).  
[17] S. Sakakibara *et al.*, Plasms Fuston Res. **1**, 049 (2006).